DOI:
10.1111/cmi.13371

Document Version
Publisher's PDF, also known as Version of record

Received: 29 January 2021 | Revised: 4 May 2021 | Accepted: 1 June 2021

DOI: 10.1111/cmi.13371

RESEARCH ARTICLE

WILEY

Candidalysin triggers epithelial cellular stresses that induce necrotic death

Mariana Blagojevic[1] | Giorgio Camilli[1] | Michelle Maxson[2] | Bernhard Hube[3,4] | David L. Moyes[1] | Jonathan P. Richardson[1] | Julian R. Naglik[1]

[1]Centre for Host-Microbiome Interactions, Faculty of Dentistry, Oral & Craniofacial Sciences, King's College London, London, UK

[2]Program in Cell Biology, Hospital for Sick Children, Toronto, Ontario, Canada

[3]Department of Microbial Pathogenicity Mechanisms, Hans-Knöll-Institute, Jena, Germany

[4]Institute of Microbiology, Friedrich-Schiller-University Jena, Jena, Germany

Correspondence
Julian R. Naglik, Centre for Host-Microbiome Interactions, Faculty of Dentistry, Oral & Craniofacial Sciences, King's College London, London SE1 1UL, UK.
Email: julian.naglik@kcl.ac.uk

Funding information
Biotechnology and Biological Sciences Research Council, Grant/Award Number: BB/N014677/1; National Institutes of Health, Grant/Award Number: R37-DE022550; Wellcome Trust, Grant/Award Number: 214229_Z_18_Z; Canadian Institutes of Health Research, Grant/Award Number: FDN-143202; Balance of the Microverse Cluster, Grant/Award Number: 390713860; German Research Foundation (Deutsche Forschungsgemeinschaft, DFG), Grant/Award Number: 528/21-1; NIH Research at Guys and St. Thomas's NHS Foundation Trust and the King's College London Biomedical Research Centre, Grant/Award Number: IS-BRC-1215-20006

Abstract

Candida albicans is a common opportunistic fungal pathogen that causes a wide range of infections from superficial mucosal to hematogenously disseminated candidiasis. The hyphal form plays an important role in the pathogenic process by invading epithelial cells and causing tissue damage. Notably, the secretion of the hyphal toxin candidalysin is essential for both epithelial cell damage and activation of mucosal immune responses. However, the mechanism of candidalysin-induced cell death remains unclear. Here, we examined the induction of cell death by candidalysin in oral epithelial cells. Fluorescent imaging using healthy/apoptotic/necrotic cell markers revealed that candidalysin causes a rapid and marked increase in the population of necrotic rather than apoptotic cells in a concentration dependent manner. Activation of a necrosis-like pathway was confirmed since *C. albicans* and candidalysin failed to activate caspase-8 and -3, or the cleavage of poly (ADP-ribose) polymerase. Furthermore, oral epithelial cells treated with candidalysin showed rapid production of reactive oxygen species, disruption of mitochondria activity and mitochondrial membrane potential, ATP depletion and cytochrome c release. Collectively, these data demonstrate that oral epithelial cells respond to the secreted fungal toxin candidalysin by triggering numerous cellular stress responses that induce necrotic death.

Take aways

- Candidalysin secreted from *Candida albicans* causes epithelial cell stress.
- Candidalysin induces calcium influx and oxidative stress in host cells.
- Candidalysin induces mitochondrial dysfunction, ATP depletion and epithelial necrosis.
- The toxicity of candidalysin is mediated from the epithelial cell surface.

Mariana Blagojevic and Giorgio Camilli contributed equally to this work.

1 | INTRODUCTION

Candida albicans is a human fungal pathogen that causes morbidity and mortality in millions of individuals worldwide each year (Brown et al., 2012). *C. albicans* possesses a multitude of virulence factors (Richardson, Ho, & Naglik, 2018) but the secretion of the peptide toxin candidalysin (encoded by the *ECE1* gene) is a key driver of cell damage and immune responses in mucosal and systemic models of *C. albicans* infection (Aggor et al., 2020; Allert et al., 2018; Drummond et al., 2019; Ho et al., 2019; Ho et al., 2020; Kasper et al., 2018; Moyes et al., 2016; Richardson et al., 2018; Richardson et al., 2018; Swidergall et al., 2019; Verma et al., 2017; Verma et al., 2018). Cell damage often results in cell stress and ultimately death, which can play a key role in host defence to microbial infections (Camilli, Blagojevic, Naglik, & Richardson, 2020; Jorgensen, Rayamajhi, & Miao, 2017). Furthermore, pathogens have evolved several strategies to induce or inhibit host cell death, aiding dissemination and survival within the host. Cell death can be driven by several biological processes including apoptosis, autophagy and different types of necrotic cell death, which can influence the outcome of a microbial insult (Camilli et al., 2020; Jorgensen et al., 2017).

Apoptosis is a highly complex form of programmed cell death, involving an energy-dependent cascade of molecular and cellular events, and can be triggered by intracellular and extracellular stimuli resulting in the activation of intrinsic and extrinsic pathways (Taylor, Cullen, & Martin, 2008). Death receptors, mitochondria and caspases drive an ordered cascade of enzymatic events that promote cell shrinkage, membrane blebbing, nuclear and cytoplasmic condensation, DNA degradation and ultimately fragmentation of the cell into apoptotic bodies, which are rapidly cleared by neighbouring phagocytes (Taylor et al., 2008). In contrast, necrotic cell death is characterised morphologically by cell and organelle swelling, loss of plasma membrane integrity and consequent inflammation. Although necrotic cell death was previously believed to result from injury, and was usually considered to be an uncontrolled process, recent evidence suggests that necrosis can also be tightly regulated (Vanden Berghe, Linkermann, Jouan-Lanhouet, Walczak, & Vandenabeele, 2014). Necroptosis, pyroptosis, ETosis, ferroptosis, parthanatos and cyclophilin D-mediated necrosis have been proposed to describe non-apoptotic cell death mechanisms that display aspects of regulated necrosis (Vanden Berghe et al., 2014).

While induction of apoptosis and necrotic cell death has predominantly been investigated in the context of viral and bacterial infections (Jorgensen et al., 2017), their importance during fungal diseases has only recently been recognised. In addition, data regarding induction or manipulation of cell death pathways during the interplay between pathogenic fungi and host cells are more limited (Camilli et al., 2020). Thus far, few components have been proposed to play a role in the induction of apoptosis in immune and non-immune cells in response to *C. albicans*. The cell-wall associated sphingolipid, phospholipomannan, can induce apoptosis in murine macrophages (Ibata-Ombetta, Idziorek, Trinel, Poulain, & Jouault, 2003), while glycan moieties (Wagener et al., 2012) and secreted aspartic proteases (Wu et al., 2013) may trigger apoptosis in oral and lung epithelial cells, respectively. However, while transcript profiling data revealed changes in the expression of apoptotic genes in oral epithelial cells after infection with live *C. albicans*, only a small fraction (10–15%) of cells exhibited mid-late apoptotic features, including loss of mitochondrial integrity, caspase-9/3 activity and DNA fragmentation (Villar, Chukwuedum Aniemeke, Zhao, & Huynh-Ba, 2012). Moreover, upregulation of anti-apoptotic genes has been observed in both epithelial cells and macrophages in response to *C. albicans* (Moyes et al., 2014; Reales-Calderon et al., 2013; Villar et al., 2012). Thus, although pro- and anti-apoptotic signalling events have been reported following in vitro stimulation of myeloid and epithelial cells with *C. albicans* or fungal components, apoptosis is a non-lytic form of cell death and cannot account for *C. albicans*–induced lysis. Live *C. albicans* induced early apoptotic signalling events in oral epithelial cells and macrophages followed by necrotic death (Panagio, Felipe, Vidotto, & Gaziri, 2002; Villar & Zhao, 2010). Furthermore, necrotic pathways that promote lytic cell death have been recently described in myeloid cells following *Candida* infection (Camilli et al., 2020; Cao et al., 2019; Kasper et al., 2018; O'Meara et al., 2015; O'Meara et al., 2018; Tucey et al., 2020; Uwamahoro et al., 2014; Vylkova & Lorenz, 2017; Wellington, Koselny, Sutterwala, & Krysan, 2014).

During infection, *C. albicans* forms hyphae, which invade tissues and induce cell death. Invasion occurs via two routes, depending on the epithelial cell type: induced endocytosis or active penetration (Dalle et al., 2010; Zakikhany et al., 2007). During the invasion, *C. albicans* causes epithelial invagination and induces an invasion pocket that is surrounded by the host cell membrane (Zakikhany et al., 2007). It is hypothesised that candidalysin is secreted into the invasion pocket, where it intercalates into host membranes to induce pore formation, which results in cell damage and ultimately, cell death (Naglik, Gaffen, & Hube, 2019). However, whether candidalysin induces epithelial cell death via apoptosis, necrosis or a combination of both mechanisms is currently unclear. Here, we provide evidence that candidalysin induces oxidative stress, mitochondrial dysfunction and epithelial cell death, which occurs predominantly via a necrotic pathway.

2 | RESULTS

2.1 | Candidalysin-induced epithelial cell death does not activate apoptosis-related caspases and occurs through a necrotic mechanism

Epithelial cell death involves physical changes to the host cell membrane and disruption of cellular homeostasis. Thus, a qualitative approach was initially used to investigate cell death features in TR146 oral epithelial cells exposed to candidalysin. Epithelial cells were treated with candidalysin at different concentrations and stained after 3, 6 and 24 h with FITC-Annexin V, EthD-III and Hoechst 33342. FITC-Annexin V produces green fluorescence when bound to phosphatidylserine residues exposed on the outer surface of the

lipid bilayer of apoptotic cells. EthD-III is unable to cross intact epithelial plasma membranes but can enter cells with damaged membranes, where it intercalates with DNA to produce red/yellow fluorescence. Hoechst 33342 (blue fluorescence) was used to visualise epithelial nuclei. As positive controls, 0.1 μM staurosporine was used to induce apoptosis (Kabir, Lobo, & Zachary, 2002) and 1% (vol/vol) Triton X-100 was used to induce cell necrosis. Fluorescence microscopy revealed markedly higher levels of necrotic cells in the population (EthD-III single positive), when compared to apoptotic cells (FITC-Annexin V single positive) or late apoptotic/necrotic cells (FITC-Annexin V/EthD-III double positive), following candidalysin stimulation (Figure 1). Plasma membrane damage, as measured by EthD-III incorporation, was observed by 3 h post stimulation with candidalysin, and increased in a concentration-dependent manner at all time points. The data indicate that candidalysin causes cytotoxicity in oral epithelial cells predominantly through necrosis.

To further investigate whether candidalysin-induced cytotoxicity was primarily due to necrosis rather than apoptosis, we analysed the processing and activity of apoptotic caspases. Caspases are cysteine-aspartic acid proteases which, when cleaved and activated, govern apoptotic cell death. Activation of caspase-8 is an essential step in the initiation of the extrinsic apoptosis pathway, while caspase-3 is the terminal caspase activated by both extrinsic and intrinsic pathways. We, therefore, examined the activation of caspase-8 and -3 in candidalysin-mediated cell death. Only epithelial cells treated with staurosporine exhibited a modest cleavage of immature caspase-8 (57 kDa) or caspase-3 (31 kDa) to produce products consistent with the molecular weight of active caspase-8 (17 kDa) and caspase-3 (19/17 kDa) (white arrows; Figure 2A, B). Since pro-caspase-8 and pro-caspase-3 were strongly expressed in epithelial cells but only modestly activated following staurosporine treatment, we also used a more sensitive luminescence-based assay to detect the presence of active caspases. Neither *C. albicans* strains nor candidalysin induced caspase-8 or caspase-3 activity in epithelial cells when compared with the vehicle control (Figure 2c). In contrast, staurosporine induced significant caspase-8 and caspase-3

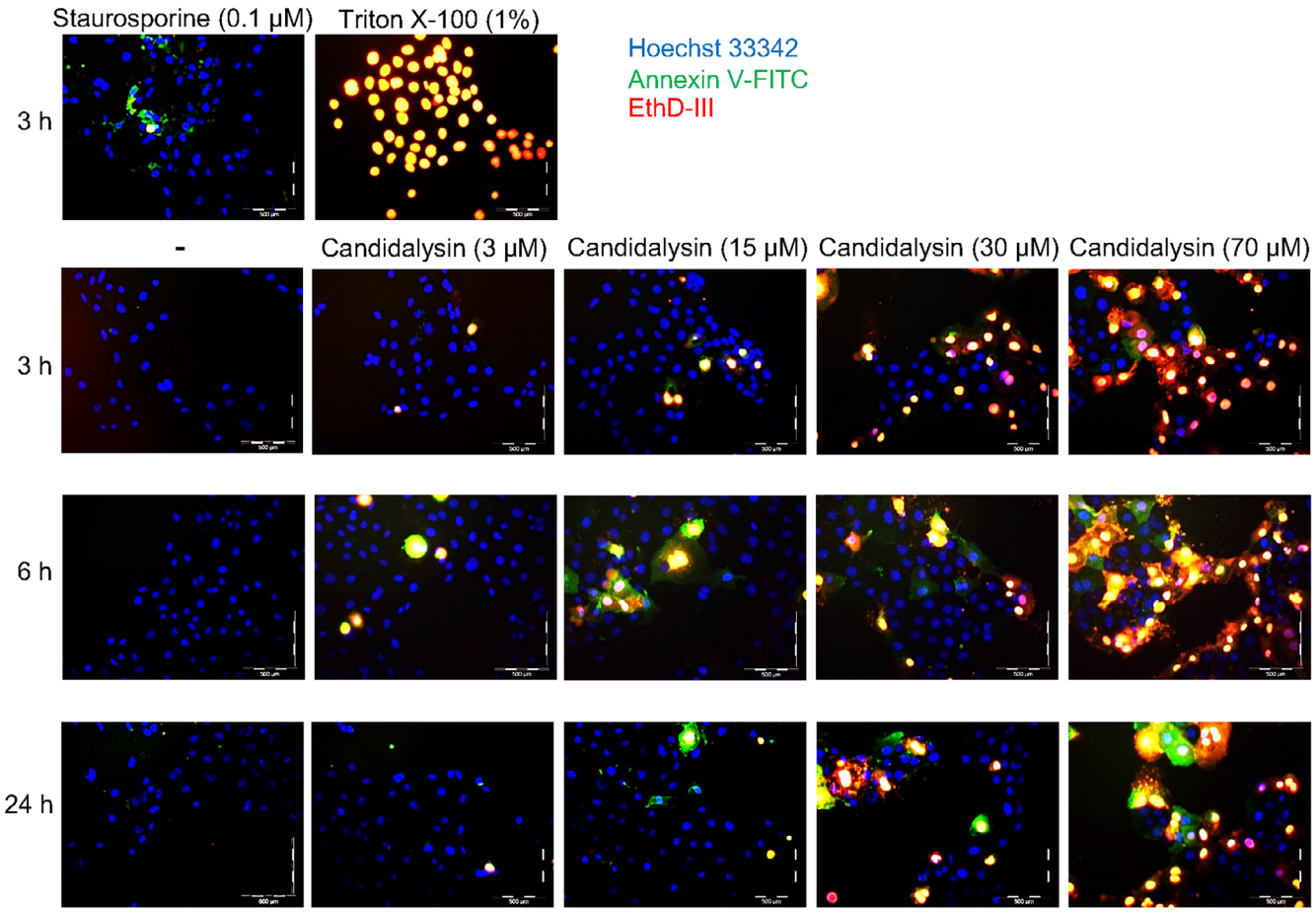

FIGURE 1 Cytotoxicity profile of candidalysin-treated epithelial cells. Fluorescence microscopy images of TR146 oral epithelial cells exposed to the indicated concentrations of candidalysin for 3, 6 and 24 h. Staurosporine and Triton X-100 were used as positive controls to induce apoptosis and necrosis, respectively. Cells were stained with Hoechst 33342 (blue: live cells), FITC-conjugated Annexin V (green: apoptotic cells) and EthD-III (red/yellow: necrotic cells). Data are representative of 3 independent experiments. Images were taken with a fluorescence microscope at ×100 magnification. Scale bars = 500 μm

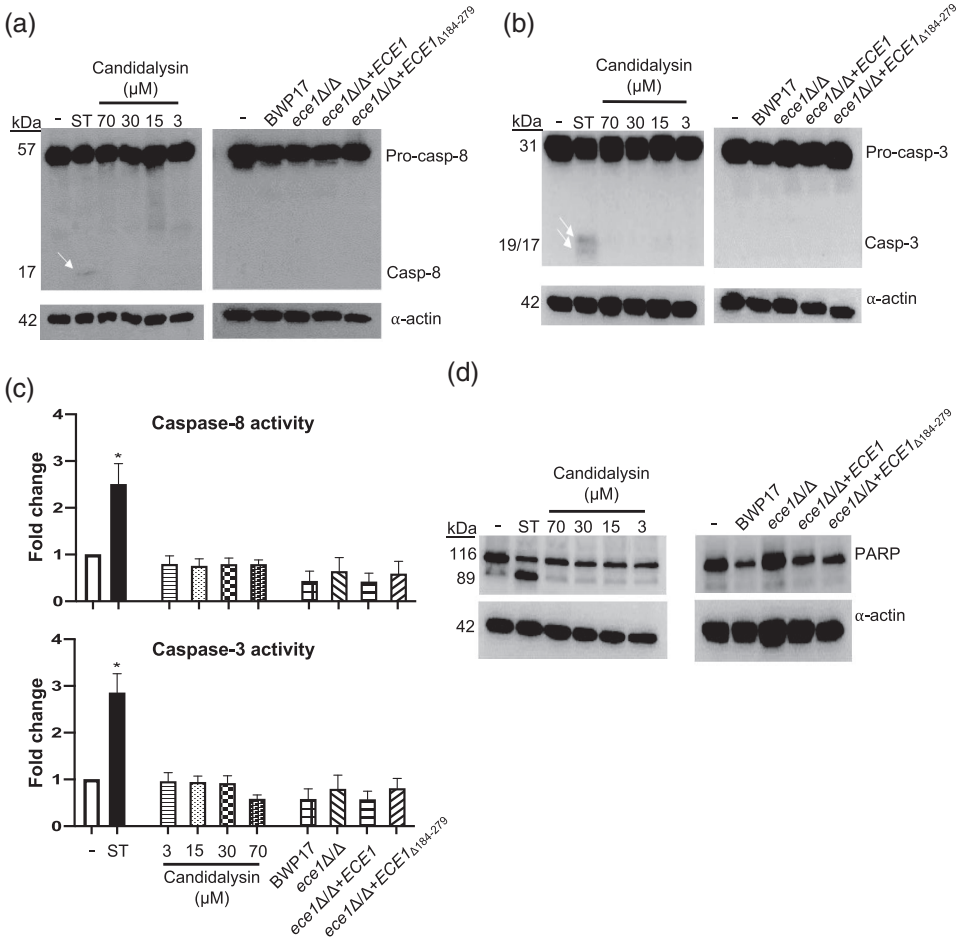

FIGURE 2 Cleavage or activation of apoptotic caspases and PARP in oral epithelial cells in response to *C. albicans* and candidalysin. (a,b) TR146 oral epithelial cells were incubated with candidalysin (70, 30, 15 and 3 μM) or live *C. albicans* (wild type and mutant strains) at a MOI of 0.01. As a positive control, 0.1 μM staurosporine was used to induce apoptosis. Total protein was isolated and analysed by SDS-PAGE and western blotting for the presence of pro-caspase/caspase-8 (a), pro-caspase/caspase-3 (b). (c) Caspase-8 and caspase-3 activity was also quantified by luminescence assay. Data represent caspase-8 and caspase-3 activity relative to the untreated control. Error bars represent mean values ± SEM of three independent experiments. *$p < .05$; one-way ANOVA. (d) Cells were treated as in (a and b), total protein was isolated and analysed by SDS-PAGE and western blotting for the presence of PARP. MOI, multiplicity of infection; PARP, poly (ADP-ribose) polymerase; SDS-PAGE, Sodium dodecyl sulphate - polyacrylamide gel electrophoresis

activity (Figure 2c). Collectively, these data demonstrate that while TR146 oral epithelial cells express high baseline levels of pro-caspase-8 and pro-caspase-3, neither *C. albicans* nor candidalysin induce the production of active caspase-8 and caspase-3 from their respective pro-caspases.

During apoptosis, poly (ADP-ribose) polymerase (PARP) is inactivated by caspase-3-mediated cleavage, which prevents DNA repair within the cell (Kaufmann & Kaufman, 1993). To confirm that a caspase-3-independent cell death mechanism was occurring in response to *C. albicans* and candidalysin, we examined the cleavage of PARP by western blot. In contrast to staurosporine, treatment of oral epithelial cells with *C. albicans* or candidalysin was not observed to induce the PARP apoptotic signature characterised by the appearance of an 89 kDa fragment (Figure 2d). Taken together, these data confirm that apoptotic events are not features of the epithelial response to *C. albicans* and candidalysin.

2.2 | Candidalysin disrupts epithelial metabolic activity and induces reactive oxygen species production and depletion of intracellular ATP

We next sought to identify the subcellular events in candidalysin-induced cell death in oral epithelial cells. We previously reported that candidalysin causes epithelial cell damage and induces calcium influx (Ho et al., 2019; Moyes et al., 2016), which are characteristics associated with cell stress and death (Cerella, Diederich, & Ghibelli, 2010). Interestingly, elevation of intracellular calcium in response to candidalysin appears to depend predominantly on calcium influx from the extracellular environment, since the toxin failed to induce an increase in intracellular calcium levels in calcium-free buffer (Figure S1). Furthermore, alterations in cellular metabolism, adenosine triphosphate (ATP) and reactive oxygen species (ROS) are common features of cytotoxicity in several cell death pathways, including necrotic death (Zong & Thompson, 2006). Accordingly, we

quantified changes in metabolism and levels of intracellular ATP and ROS in response to candidalysin.

Epithelial cells were treated with candidalysin for 3 h and metabolic activity was quantified by MTT assay. Concentrations of candidalysin greater than 15 μM induced a significant decrease in cellular metabolism (Figure 3a). A more detailed time course experiment revealed that lytic (70 μM) and borderline-lytic (15 μM) concentrations of candidalysin caused a 75 and 50% reduction in metabolic

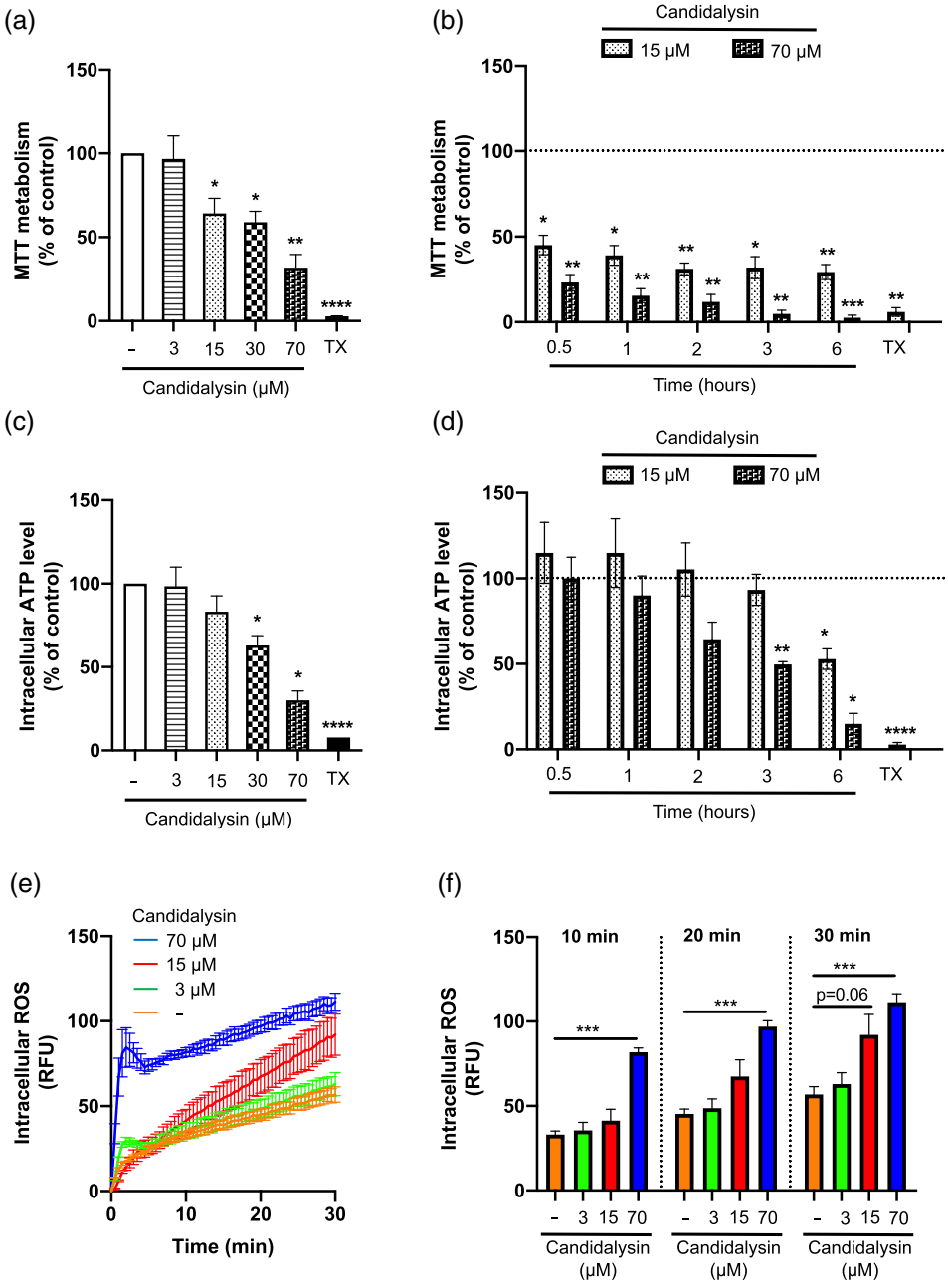

FIGURE 3 Candidalysin induces loss of metabolic activity, depletion of intracellular ATP and accumulation of intracellular reactive oxygen species (ROS). (a) TR146 oral epithelial cells were treated with candidalysin (3, 15, 30, 70 μM) for 3 h and assayed for metabolic activity by MTT assay. (b) Time-course experiments (0.5–6 h) of TR146 oral epithelial cells treated with candidalysin at 70 or 15 μM and assayed for metabolic activity by MTT. (c) TR146 oral epithelial cells were treated with candidalysin (3, 15, 30, 70 μM) for 3 h and assayed for intracellular ATP by luminescence assay. (d) Time-course experiments (0.5–6 h) of TR146 oral epithelial cells treated with candidalysin at 70 or 15 μM and assayed for intracellular ATP by luminescence assay. Triton X-100 (1%) (TX) was used as a positive control. Data are expressed as a percentage of metabolic activity or intracellular ATP in comparison with the untreated control. Error bars represent mean values ± SEM of three independent experiments. (e) To assess the production of intracellular ROS, TR146 oral epithelial cells were pre-incubated with DCFH-DA for 1 h and subsequently incubated with candidalysin (70, 15 and 3 μM). Fluorescence was measured in real time over 30 min. Data are expressed as relative fluorescence units (RFU). (f) RFU data at 10, 20 and 30 min are plotted as histograms of mean ± SEM of ROS production corresponding to three independent experiments. * $p < .05$, ** $p < .01$, *** $p < .001$, **** $p < .0001$; one-way analysis of variance

activity respectively within 0.5 h, which was further decreased by 95% at 6 h in response to 70 μM candidalysin (Figure 3b).

Since epithelial cells treated with candidalysin exhibited cellular hallmarks of necrosis (Figure 1), and reductions in the cellular energy pool predispose cells to necrotic-like cell death (Zong & Thompson, 2006), we next assessed levels of intracellular ATP. Compared with untreated epithelial cells, exposure to lytic concentrations of candidalysin (≥30 μM) resulted in a significant decrease in the level of intracellular ATP (Figure 3c). Further analysis revealed that ATP depletion proceeded in a dose- and time-dependent manner (Figure 3d).

Since the accumulation of ROS is associated with necrotic death (Zong & Thompson, 2006), we next examined whether candidalysin treatment could induce oxidative stress in epithelial cells. Candidalysin induced the production of ROS in a time- and concentration-dependent manner (Figure 3e,f). The level of ROS peaked sharply (within 5 min) in response to 70 μM candidalysin and reached a maximum at 30 min post treatment. Epithelial cells treated with 15 μM candidalysin exhibited a gradual increase in ROS which reached marginally significant levels ($p = .06$) at 30 min (Figure 3e,f).

Collectively, these data indicate that candidalysin induces a loss of metabolic activity, depletion of ATP and oxidative stress in epithelial cells which is closely associated with a necrotic cell death mechanism.

2.3 | Candidalysin causes mitochondrial dysfunction and cytochrome c release during *C. albicans* infection

Mitochondria play a pivotal role in the production of energy (e.g., ATP) and mitochondrial dysfunction is a central feature of both apoptotic and necrotic cell death (Baines, 2010; Wang, 2001). Therefore, we investigated whether loss of mitochondrial membrane potential (ΔΨm) and/or loss of mitochondrial membrane integrity occurs in epithelial cells in response to candidalysin. We used rhodamine 123 (a green fluorescent dye that selectively accumulates in mitochondria in a membrane potential-dependent manner) and confocal microscopy to visualise changes in mitochondrial potential induced by *C. albicans* and candidalysin. A concentration of 30 μM candidalysin was chosen to minimise membrane permeability, cell swelling and detachment, rapidly and robustly induced by higher concentration of the toxin (e.g., 70 μM).

Epithelial cells treated with 30 μM candidalysin exhibited a reduction in ΔΨm compared with untreated control cells (Figure 4a). Since candidalysin induces robust calcium influx (Ho et al., 2019; Moyes et al., 2016), and calcium levels affect mitochondrial dynamics (Finkel et al., 2015), we also conducted experiments in a calcium free buffer. Notably, candidalysin-induced mitochondria depolarization was inhibited in the absence of calcium, strongly suggesting that the toxin induces changes in mitochondrial membrane potential in response to increasing levels of cytosolic calcium (Figure 4a). Similarly, we found that mitochondria depolarization was markedly higher following infection of oral epithelial cells with wild type *C. albicans* as compared with a candidalysin deficient *C. albicans* strain (*ece1*Δ/Δ; Figure 4b). Interestingly, it appears that candidalysin mediates its effects on mitochondria from the epithelial surface, as an AlexaFluor 647-labelled candidalysin (also damaging) remained in the plasma membrane and did not enter the epithelial cell (Figure 4c). Taken together, these data demonstrate that during epithelial infection, candidalysin induces significant cell stress by affecting mitochondrial dynamics in a calcium-dependent manner.

Dysfunctional mitochondria release proteins including cytochrome c that amplify intracellular caspase cascades during apoptosis. However, release of cytochrome c into the cytosol also occurs during necrotic cell death (Li, Li, Pinto, & Pardee, 1999). Moreover, the rapid disappearance of cytochrome c from dying cells has been attributed to its release into the extracellular environment (Jemmerson, LaPlante, & Treeful, 2002). Therefore, although we observed no caspase activation in candidalysin-mediated cell death, the loss of mitochondrial membrane potential following candidalysin treatment prompted us to investigate whether cytochrome c is released from epithelial cells.

Epithelial cells were treated with candidalysin or *C. albicans* strains and the level of cytochrome c was quantified in exhausted culture medium. Treatment with staurosporine, used as a positive control, induced significant release of cytochrome c into the extracellular environment (Figure 4d). Candidalysin-treated cells also exhibited a trend towards increased cytochrome c release compared to controls ($p = .05$; Figure 4d). Importantly, when epithelial cells were infected with live fungus, significant levels of cytochrome c were released only following stimulation with candidalysin producing *C. albicans* strains (wild type, *ece1*Δ/Δ + *ECE1*) as compared with candidalysin-deficient strains (*ece1*Δ/Δ, *ece1*Δ/Δ + $ECE1_{\Delta 184-279}$; Figure 4e), suggesting that candidalysin contributes to cytochrome c release from epithelial cells during *C. albicans* infection.

3 | DISCUSSION

Cytolytic proteins and peptide toxins are classical virulence factors that disrupt epithelial barrier function, damage cells and activate or modulate host immune responses. As such, a better understanding of how toxins damage and kill host cells may provide valuable insights into both pathogenicity mechanisms and antimicrobial immune responses. Toxin-induced host cell death can be driven by several biological processes including apoptosis and necrosis, which can influence the outcome of a microbial infection (Camilli et al., 2020; Jorgensen et al., 2017). Candidalysin is the first, and currently only, peptide toxin identified in any human fungal pathogen (Moyes et al., 2016). We and others have shown that candidalysin causes cell damage and is critical for *C. albicans* pathogenicity in mucosal and systemic infection models (Aggor et al., 2020; Allert et al., 2018; Drummond et al., 2019; Ho et al., 2019; Ho et al., 2020; Kasper et al., 2018; Moyes et al., 2016; Richardson, Mogavero, et al., 2018; Richardson, Willems, et al., 2018; Swidergall et al., 2019; Verma et al., 2017;

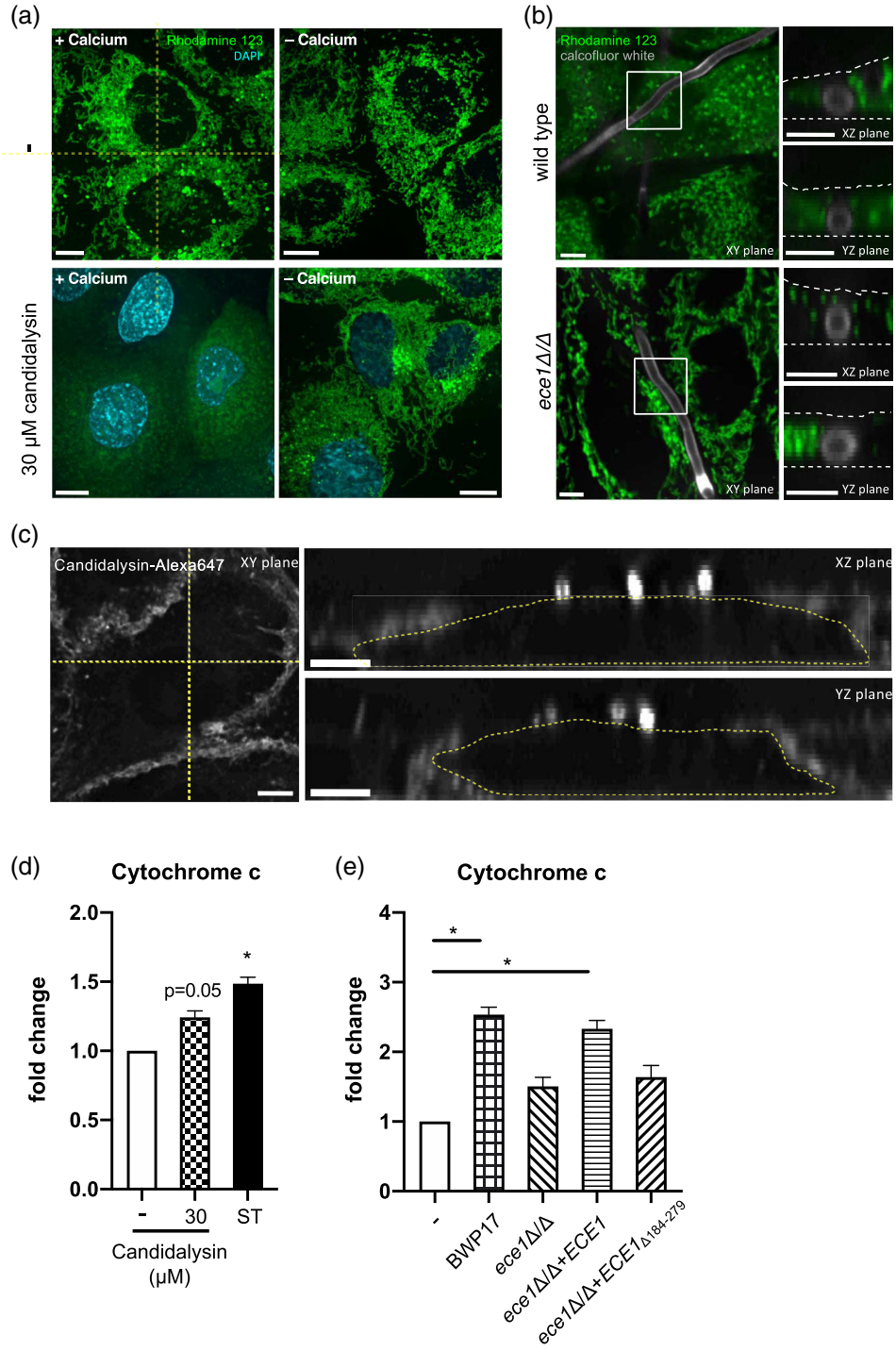

FIGURE 4 Candidalysin induces loss of mitochondrial membrane potential and cytochrome c release. (a) Epithelial cells were pre-labelled with Rhodamine 123 (green) and incubated with candidalysin/control peptide in the presence or absence of calcium then visualised by confocal microscopy in the presence of DAPI (cyan). Images are maximum projections representative of ≥30 fields from three independent experiments. Scale bars = 10 μm. (b) Following *C. albicans* invasion, TR146 cells pre-labelled with Rhodamine 123 (green) were stained 5 min with 10 μg/ml calcofluor white (to label *C. albicans*; white) and visualised by confocal microscopy. Diffuse green images indicate a reduction in mitochondrial potential. Images are central optical slices representative of ≥15 fields from two separate experiments. The white solid box within *XY* optical slice indicates location of accompanying *XZ* and *YZ* reconstructions (right). *XZ* and *XY* images of invading *C. albicans* indicate the upper and lower bounds of epithelial plasma membrane, visualised by brightfield microscopy, with dotted white lines. Scale bars = 5 μm. (c) Candidalysin exerts its effects while localised at the plasma membrane of epithelial cells. After incubation with candidalysin-Alexa 647, TR146 cells were visualised by confocal microscopy. Candidalysin-Alexa 647 shown in white. The location of the plasma membrane, visualised by brightfield microscopy, is indicated by a dotted yellow line. Left image is a central *XY* slice; yellow dotted crosshairs within image indicate the locations of accompanying *XZ* (horizontal line) and *YZ* (vertical line) slices (displayed to the right). Images are optical slices representative of ≥10 fields from two separate experiments. Scale bars = 5 μm. (d, e) TR146 oral epithelial cells were incubated with 30 μM candidalysin or live *C. albicans* (wild type and mutant strains) at a multiplicity of infection of 0.01. Staurosporine (0.1 μM) was used as positive control. Cytochrome c was quantified in exhausted culture medium by ELISA. Data are expressed as fold change of cytochrome c levels comparison to the untreated control. Error bars represent mean values ± SEM of three independent experiments. Significant differences relative to the untreated control: * $p < .05$; one-way analysis of variance. ELISA, enzyme linked enzyme-linked immunoassay

Verma et al., 2018). Toxin-induced cell damage results in cell stress, activation of immune responses and ultimately cell death. While *C. albicans* is known to induce both necrotic and apoptotic cell death mechanisms in human cells (Camilli et al., 2020), the role of candidalysin in driving these responses was unclear. Using an in vitro model of intestinal translocation, *C. albicans* was observed to associate with fungus-induced necrotic, but not apoptotic, intestinal epithelial cell death (Allert et al., 2018). Importantly, candidalysin was observed to cause enterocyte damage, which correlates with fungal translocation (Allert et al., 2018). Here, we demonstrate that *C. albicans*/candidalysin damages human oral epithelial cells in a manner that is independent of apoptotic caspases, but which exhibits several hallmarks of necrotic death. Furthermore, we provide new insight into the mechanisms by which candidalysin may orchestrate a necrotic response in epithelial cells.

Multiple cellular assays demonstrated that lytic concentrations of candidalysin induce a necrotic effect and appears to target mitochondrial function, as evidenced by decreased metabolic activity, depletion of intracellular ATP and an increase in the level of intracellular ROS. The effect on mitochondria was further confirmed by confocal microscopy which revealed destabilisation of mitochondrial membrane potential when epithelial cells were exposed to wild type *C. albicans* or candidalysin, but not with a *C. albicans* strain unable to produce candidalysin. Notably, candidalysin was not observed to enter epithelial cells during the 10 min analysis period, suggesting that the toxin mediates its effects from the cell surface. Furthermore, these cellular effects were only observed in the presence of calcium. Given that calcium influx is a key feature of candidalysin function (Ho et al., 2019; Moyes et al., 2016), we propose that candidalysin-induced pore formation results in mitochondrial dysfunction in a calcium dependent manner, which ultimately affects cell fate.

While candidalysin damages oral epithelial cells (Moyes et al., 2016) and promotes cell death by necrosis (this study), previous work by *Allert* et al. has demonstrated that a combination of hypha formation and candidalysin secretion is required for optimal damage of intestinal epithelial cells by *C. albicans* (Allert et al., 2018). This discrepancy is likely caused by differences in the susceptibility of epithelial cell types to harmful stimuli and pathogens. For instance, the ability of *C. albicans* to adhere to and invade human epithelial cells clearly differs between enterocytes and oral epithelial cells (Dalle et al., 2010), and the presence of tight junctions was demonstrated to play a key role in the protection of enterocytes against *C. albicans* invasion (Goyer et al., 2016). Moreover, the mechanism of *C. albicans* mucosal invasion is different between tissues: intestinal invasion is achieved through active penetration, while a combination of active penetration and receptor-induced endocytosis occurs during oral invasion (Dalle et al., 2010), which may influence the nature of the invasion pocket and, ultimately, the effectiveness of the toxin. Therefore, although the mechanism by which candidalysin induces epithelial cell death may be similar, the presence and extent of epithelial necrosis may differ in distinct cells or anatomical niches.

The death of immune effector cells by both intrinsic and extrinsic apoptotic pathways may dampen host antifungal responses and has been shown to occur during fungal infections, most notably with *Aspergillus* and *Cryptococcus* (Camilli et al., 2020). However, the activation and role of apoptosis during *Candida* infection remains unclear, and the induction of both apoptosis and survival pathways has been reported (Camilli et al., 2020). Early apoptotic events have been described in macrophages in response to the highly virulent CR1 strain of *C. albicans* in vitro and in vivo (Gasparoto, Gaziri, Burger, de Almeida, & Felipe, 2004; Panagio et al., 2002). However, phagocytosis of CR1 yeast cells induced early apoptotic events before germ tube formation and subsequent lysis of macrophages by necrosis (Panagio et al., 2002). Consistent with the findings from macrophages, live *C. albicans* induced early apoptotic signalling events in oral epithelial cells followed by necrotic death (Villar & Zhao, 2010). Only a modest increase of caspase-3 and -9 (but not caspase-8) activity was observed during the early stages of infection, which returned to levels similar to those observed in uninfected cells at later time points (Villar & Zhao, 2010). The morphological transition from yeast to hyphae is, therefore, likely to play a crucial role in the inhibition of apoptotic progression and induction of a lytic cell death mechanism. Accordingly, our data indicate that oral epithelial cells do not undergo pro-apoptotic changes in response to the hyphal toxin candidalysin.

Our study describes the responses of a human buccal squamous cell carcinoma cell line to *C. albicans* and candidalysin. Although one of the hallmarks of cancer cells is resistance to apoptosis, several studies have demonstrated that TR146 cells are capable of undergoing apoptosis (Han et al., 2015; O'Callaghan et al., 2015; Wagener et al., 2012). Similarly, in the present study, we demonstrate that staurosporine induces annexin V binding, caspase-3 and -8 activation and cleavage of PARP in TR146 cells. However, the cells were most intensively stained with EthD-III following candidalysin treatment, and candidalysin did not induce caspase-3 or -8 processing, or detectable caspase activity at any concentration tested. These data suggest that cell death proceeds through a lytic but non-apoptotic mechanism. Recent research with vaginal epithelial cells further corroborate these findings (Pekmezovic et al., 2021). Staurosporine was observed to trigger apoptosis in both primary vaginal cells and a vaginal epithelial carcinoma cell line, while the level of apoptosis was not observed to differ between *Candida* infected and uninfected cells (Pekmezovic et al., 2021). Moreover, primary mononuclear phagocytes undergo necrotic cell death in response to candidalysin with only minimal exposure of cell surface phosphatidylserine (Annexin V-positive cells) in the absence of pro-apoptotic caspase activation (Kasper et al., 2018). A similar mechanism may, therefore, contribute to candidalysin-induced cell death in both myeloid and epithelial cells.

Of note, cell swelling, organelle dysfunction and rupture of the plasma membrane have recently been recognised as features of cell death mechanisms that are similar to necrosis, but which are regulated by specific intracellular signalling programmes (Vanden Berghe et al., 2014). Thus far, while the activation of such regulated necrotic mechanisms has been reported in myeloid cells in response to *C. albicans* (Camilli et al., 2020), these molecular pathways have not yet been identified in epithelial cells. For instance, *C. albicans* can trigger macrophage cell death via the necroptotic pathway in the absence of caspase-8 activity (Cao et al., 2019), and several independent studies have demonstrated the ability of *C. albicans* to induce NLRP3

inflammasome-dependent pyroptosis (Camilli et al., 2020; O'Meara et al., 2015, 2018; Tucey et al., 2020; Uwamahoro et al., 2014; Wellington et al., 2014). However, although candidalysin activates the NLRP3 inflammasome and induces cytolysis in both murine and human mononuclear phagocytes, cell death appears to be independent of inflammasome activation, as demonstrated by the use of a caspase-1 inhibitor or mononuclear phagocytes isolated from mice lacking NLRP3 or caspase-1 (Kasper et al., 2018). Furthermore, the necroptosis inhibitor necrostatin-1 did not inhibit the cytolytic effect of candidalysin (Kasper et al., 2018), suggesting that neither necroptosis nor pyroptosis contribute to candidalysin-driven macrophage cell death. Whether *C. albicans*/candidalysin kills macrophages through a different regulated necrotic pathway and whether the cell death mechanism is conserved between myeloid and non-myeloid cells remains to be determined.

It is now widely accepted that mitochondria represent a central control point not only during apoptosis but also for the execution of necrotic cell death programmes (Baines, 2010). Numerous studies have suggested that calcium overload and oxidative stress lead to the opening of a channel in the mitochondria inner membrane, termed the mitochondrial permeability transition pore (mPTP), which results in a dramatic depolarization of $\Delta\Psi m$ and release of proteins and solutes including apoptogenic factors (Bauer & Murphy, 2020). Notably, a sustained and prolonged mPTP opening is associated with the loss of mitochondrial membrane potential, cessation of ATP synthesis, mitochondrial swelling, rupture and necrotic cell death (Ying & Padanilam, 2016). Indeed, while apoptosis is an ATP-dependent process, necrosis is ATP-independent and therefore, a high proportion of damaged mitochondria and ATP depletion are likely to promote necrotic, but not apoptotic cell death (Ying & Padanilam, 2016). Similarly, our data establish that candidalysin secretion by *C. albicans* is the key trigger of cell death in epithelial cells, a process that is closely linked to calcium influx, oxidative stress, mitochondrial dysfunction and decreased metabolic activity. As such, the implications of mitochondrial dysfunction in candidalysin-induced cell death may be of particular interest for future investigations.

In summary, this study demonstrates that candidalysin induces a specific pro-death pathway from the cell surface that converges on mitochondria to regulate a necrotic cell death program in epithelial cells. Further studies will be necessary to identify the precise molecular pathways that promote the alteration of mitochondrial physiology in epithelial cells during *C. albicans*/candidalysin infection.

4 | EXPERIMENTAL PROCEDURES

4.1 | Cell culture

The TR146 human buccal epithelial squamous cell carcinoma cell line (Rupniak et al., 1985) was obtained from the European Collection of Authenticated Cell Cultures (ECACC). TR146 cells were cultured in Dulbecco's Modified Eagle Medium/F-12 (DMEM/F12) Nutrient Mixture (1:1) + L-glutamine (Life Technologies) supplemented with 15% (vol/vol) heat-inactivated foetal bovine serum (Life Technologies) and 1% (vol/vol) penicillin–streptomycin (Sigma) at 37°C, 5% CO_2. For cell damage, enzyme linked enzyme-linked immunoassay (ELISA) and western blotting assays, the culture medium was replaced 24 h prior to experimentation with serum-free medium and maintained until the cells were harvested.

4.2 | *C. albicans* strains

All *C. albicans* strains used in this study were generated previously (Moyes et al., 2016) and are listed in Table 1. *C. albicans* cells were cultured in liquid yeast peptone dextrose (YPD), consisting of 1% (wt/vol)

TABLE 1 *Candida albicans* strains used in this study

Name	Description	Genotype[a]
BWP17+Clp30	Parental wild type *C. albicans* strain	*ura3*::λ*imm434*/*ura3*::λ*imm434* *iro1*::λ*imm434*/*iro1*::λ*imm434* *his1*::*hisG*/*his1*::*hisG* *arg4*::*hisG*/*arg4*::*hisG* *RPS1*/*rps1*::(*URA3-HIS1-ARG4*)
*ece1*Δ/Δ	*C. albicans* mutant strain with the *ECE1* gene deleted	*ura3*::λ*imm434*/*ura3*::λ*imm434* *iro1*::λ*imm434*/*iro1*::λ*imm434* *his1*::*hisG*/*his1*::*hisG* *arg4*::*hisG*/*arg4*::*hisG* *ece1*::*HIS1*/*ece1*::*ARG4* *RPS1*/*rps1*::(*URA3*)
*ece1*Δ/Δ+*ECE1*$_{\Delta 184-279}$	*C. albicans* mutant strain with only the candidalysin encoding region of *ECE1* deleted	*ura3*::λ*imm434*/*ura3*::λ*imm434* *iro1*::λ*imm434*/*iro1*::λ*imm434* *his1*::*hisG*/*his1*::*hisG* *arg4*::*hisG*/*arg4*::*hisG* *ece1*::*HIS1*/*ece1*::*ARG4* *RPS1*/*rps1*::(*URA3-ECE1*$_{\Delta 184-279}$)
*ece1*Δ/Δ+*ECE1*	*C. albicans* revertant strain with the *ECE1* gene recomplemented	*ura3*::λ*imm434*/*ura3*::λ*imm434* *iro1*::λ*imm434*/*iro1*::λ*imm434* *his1*::*hisG*/*his1*::*hisG* *arg4*::*hisG*/*arg4*::*hisG* *ece1*::*HIS1*/*ece1*::*ARG4* *RPS1*/*rps1*::(*URA3-ECE1*)

[a]All *C. albicans* strains used were prototrophic for histidine, arginine and uridine, achieved by genomic integration of Clp30 (containing *HIS1*, *ARG4* and *URA3*) genes.

yeast extract (Oxoid), 2% (wt/vol) Peptone (Melford), 2% (wt/vol) dextrose (BDH Chemicals) and 1.5% (wt/vol) agar (Melford) at 30°C overnight in a shaking incubator (180 rpm) to reach saturation. Cultures were washed in sterile PBS and adjusted to the required cell density. For cell damage, ELISA and western blotting assays, epithelial cells were infected with *C. albicans* strains at a multiplicity of infection (MOI) of 5 for 6 h and a MOI of 0.01 for 24 h. Following infection, cells were cultured at 37°C, 5% CO_2.

4.3 | Candidalysin

Candidalysin (SIIGIIMGILGNIPQVIQIIMSIVKAFKGNK) was synthesised and purified (>95% purity) by Peptide Protein Research Ltd. (UK) and was reconstituted to a stock concentration of 10 mg/ml (3 mM) in water and stored at −20°C. For experimentation, candidalysin was used at lytic (≥30 μM), borderline-lytic (15 μM) and sublytic (≤3 μM) concentrations, as previously determined (Ho et al., 2019; Moyes et al., 2016).

4.4 | Western blotting

Whole cell lysates were collected by washing cells with ice cold D-PBS and lysing cells in modified RIPA buffer [50 mM Tris–HCl (pH 7.4), 150 mM NaCl, 1 mM EDTA, 1% Triton X-100, 1% sodium deoxycholate, 0.1% SDS] containing protease (Sigma-Aldrich) and phosphatase (Perbio Science) inhibitors. After incubation on ice for 30 min, the crude lysate was clarified by centrifugation at 20,000*g*, 4°C for 10 min. Lysate supernatants were assayed for total protein content using a BCA protein quantitation kit (Perbio Science). Proteins were separated on 12% SDS-PAGE gels before transfer to nitrocellulose membranes (GE Healthcare). Following transfer, membranes were incubated on a shaker for 1 h in a blocking solution (5% dry milk prepared in 1X TBS-T) and were subsequently incubated with primary antibodies (1:1,000) and secondary IgG horseradish peroxidase (HRP)-conjugated antibodies (Jackson ImmunoResearch; 1:10,000). Target proteins were detected by incubating membranes in a chemiluminescent solution (Immobilon Western, Chemiluminescent Substrate; Millipore) for 5 min and exposing the membrane to film (GE Healthcare Life Sciences). Caspase-8, Caspase-3 and PARP primary antibodies were purchased from Cell Signalling. Alpha-actin (Millipore) was used as a loading control.

4.5 | Cell death by fluorescent microscopy

Epithelial cell death was investigated using the Apoptotic/Necrotic/Healthy Cell Detection Kit (Promokine). Briefly, treated cells were washed twice with 5X binding buffer. Staining solution (5 μl FITC-Annexin V, 5 μl Ethidium Homodimer III [EthD-III] and 5 μl of Hoechst 33342 in 100 μl 5X Binding Buffer) was added to cells and incubated for 15 min at room temperature protected from light. Cells were washed once with 5X binding buffer and images were acquired using an Olympus CKX41 inverted microscope using fluorescein isothiocyanate (FITC), Texas Red and 4′,6-diamidino-2-phenylindole (DAPI) filter sets with ×10 magnification. As positive controls, 0.1 μM staurosporine (Sigma) was used to induce apoptosis and 1% (vol/vol) Triton X-100 (Sigma) was used to induce cell necrosis.

4.6 | Mitochondrial fitness by MTT assay

3-(4,5-dimethylthiazol-2-yl)-2,5-diphenyltetrazolium bromide (MTT) (Merck) was prepared to 5 mg/ml in PBS and sterilised through a 0.2 μm filter. Control and treated cells were incubated with 20 μl of yellow MTT solution at 37°C for 3 h. This was followed by the addition of 150 μl of MTT solubilisation solution consisting of 50% dimethylformamide (Prolabo), 0.2% glacial acetic acid (BDH Chemicals), 20 mM hydrochloric acid (HCl; BDH Chemicals), 10% (wt/vol) sodium dodecyl sulfate (SDS; Severn Biochem Ltd.) and incubated overnight at 37°C. Absorbance was measured at 620 nm wavelength using a Tecan Infinite F50 plate reader. Values were calculated as a percentage of the untreated control.

4.7 | Detection of intracellular ROS

Intracellular ROS was measured using an OxiSelect Intracellular ROS Assay Kit (Cell Biolabs) according to the manufacturer's protocol. Briefly, culture medium was collected and 50 μl of 2′,7′-Dichlorodihydrofluorescin diacetate (DCFH-DA) solution (20X DCFH-DA stock diluted in 1X DMEM/F-12 media) was added and the plate incubated for 1 h at 37°C, 5% CO_2. The DCFH-DA solution was replaced with 50 μl D-PBS and baseline fluorescence readings (excitation 480 nm/emission 530 nm) were taken for 10 min using a FlexStation 3 (Molecular Devices). Following cell treatment, readings were taken immediately for up to 30 min. Data were analysed using Softmax Pro software.

4.8 | Detection of intracellular ATP

Intracellular ATP was measured using a CellTiter-Glo Luminescent Cell Viability Assay (Promega) according to the manufacturer's protocol. Briefly, a substrate solution containing luciferin and inactive luciferase (CellTiter-Glo Reagent) was added to control and treated cells (1:1 ratio of CellTiter-Glo Reagent volume to sample volume). Catalytic oxidation of luciferin by luciferase in the presence of cellular ATP, Mg^{2+} and molecular oxygen generates a luminescent signal which is proportional to the amount of ATP present within the cells. Luminescence was measured using a FlexStation 3 (Molecular Devices) and data analysed using Softmax Pro software.

4.9 | Imaging of mitochondrial potential

Rhodamine 123 staining was utilised to visualise mitochondrial potential by confocal microscopy (Baracca, Sgarbi, Solaini, & Lenaz, 2003).

One day prior to experiments, TR146 cells were seeded onto 18 mm glass coverslips at a concentration of 1 x 10^5 cells/ml in DMEM/F12 medium and incubated for 16 h at 37°C, 5% CO_2. The next day, cells were washed with 1X PBS and incubated in isotonic minimal media containing calcium (140 mM NaCl, 3 mM KCl, 1 mM $CaCl_2$, 1 mM $MgCl_2$, 15 mM HEPES, 5 mM glucose; pH 7.4) and 1 μg/ml Rhodamine 123 (Sigma Aldrich) for 15 min at 37°C. After mitochondrial labelling with Rhodamine 123, cells were treated as follows. For treatment with candidalysin, monolayers were washed three times with 1X PBS without calcium and magnesium, and incubated for 10 min in the presence or absence of 30 μM candidalysin in isotonic media ± calcium. Following treatments, monolayers were incubated in fresh isotonic minimal media ± calcium containing 5 μg/mL DAPI (Sigma Aldrich) for 5 min at 37°C and viewed live. For treatments of labelled TR146 cells with *C. albicans* strains, monolayers were washed three times with 1X PBS with calcium and magnesium, and medium replaced with isotonic minimal media containing calcium. Log-phase *C. albicans* was added to monolayers at an MOI of 0.25; the plates were then centrifuged for 1 min at 1500 rpm and incubated for 4 h at 37°C. Following invasion, coverslips were stained for 5 min with 10 μg/ml calcofluor white to label *C. albicans* and coverslips were viewed live.

4.10 | Imaging of candidalysin-Alexa647 treated cells

- One day prior to experiments, TR146 cells were seeded onto 18 mm glass coverslips at a concentration of 1 x 10^5 cells/ml in DMEM/F12 supplemented with L-glutamine and 10% heat-inactivated foetal calf serum, and incubated 16 h at 37°C, 5% CO_2. The following day, cells were washed with 1X PBS and incubated in isotonic minimal media containing calcium. Synthetic candidalysin-Alexa647, previously resuspended to a concentration of 1.4 mM in sterile dH_20, was cup sonicated in ice water for 5–60 s intervals to obtain a homogeneous suspension. TR146 monolayers were then incubated with 30 μM candidalysin-Alexa647 for 10 min at 37°C. After incubation, cells were washed three times with 1X PBS and fixed in 4% paraformaldehyde for 10 min at room temperature. Fixative was replaced with 1X PBS and coverslips viewed by confocal microscopy.

4.11 | Confocal microscopy and image analysis

Confocal images were acquired using a Yokogawa CSU10 spinning disk system (Quorum Technologies, Inc.). The imaging system is based on an Axiovert 200M microscope (Zeiss) equipped with a 63×/1.4 NA oil objective (Zeiss), and an additional ×1.5 magnifying lens. The microscope carries a motorised XY stage (Applied Scientific Instrumentation), a Piezo Z-focus drive, and diode-pumped solid-state lasers emitting at 440, 491, 561, 638 and 655 nm (Spectral Applied Research). Images were recorded with a back-thinned, cooled charge-coupled device camera (Hamamatsu Photonics) and Volocity software (version 6.2.1; Quorum Technologies, Inc.). For live experiments, cells were maintained at 37°C using an environmental chamber (Live Cell Instruments). Routine image analyses were performed using Volocity software.

4.12 | Quantification of cytochrome c

Exhausted cell culture medium was quantified for cytochrome c using the Cytochrome c human ELISA kit (Invitrogen) according to the manufacturer's instructions. Determination of cytochrome c concentration was performed by measuring absorbance at 450 nm using a Tecan Infinite F50 plate reader.

4.13 | Detection of caspase activity

Caspase-3 and Caspase-8 activity was measured using a Caspase-Glo 3/7 and Caspase-Glo 8 Assay (Promega), according to the manufacturer's protocol. Briefly, a solution containing a cell lysis reagent and a quenched (non-luminescent) caspase-specific substrate was added to control and treated cells (1:1 ratio of assay reagent volume to sample volume). Luminescence was measured after a 30 min incubation with substrate for caspase-3 and 1 h incubation for caspase-8 using a FlexStation 3 (Molecular Devices). Data was analysed using Softmax Pro software.

4.14 | Statistical analysis

The significance level was determined by one-way analysis of variance (ANOVA) with Dunnett's correction for multiple comparisons. A difference was considered statistically significant at $p < .05$. At least three independent biological replicate experiments were performed. Data were analysed using GraphPad Prism, version 8.0 (GraphPad Software) and are shown as the mean ± SEM.

ACKNOWLEDGEMENTS

This work was supported by grants from the Wellcome Trust (214229_Z_18_Z), Biotechnology & Biological Sciences Research Council (BB/N014677/1), National Institutes of Health (R37-DE022550) and the NIH Research at Guys and St. Thomas's NHS Foundation Trust and the King's College London Biomedical Research Centre (IS-BRC-1215-20006) to Julian R. Naglik. Bernhard Hube was supported by German Research Foundation (Deutsche Forschungsgemeinschaft, DFG) project Hu 528/21-1 and the Balance of the Microverse Cluster (Germany's Excellence Strategy – EXC 2051 – Project-ID 390713860). M.M. was the recipient of a Heart and Stroke Pfizer Research Fellowship and is currently supported on Canadian Institutes of Health Research grant FDN-143202.

CONFLICT OF INTEREST

The authors declare no conflicts of interest.

AUTHOR CONTRIBUTIONS

Mariana Blagojevic, Jonathan P. Richardson and Julian R. Naglik: Conceived the study. **Mariana Blagojevic and Michelle Maxson:**

Performed experiments. **Giorgio Camilli, Mariana Blagojevic, Jonathan P. Richardson, Michelle Maxson and Julian R. Naglik:** Analysed and interpreted the data. **Giorgio Camilli, Mariana Blagojevic and Julian R. Naglik:** Wrote the manuscript. **Giorgio Camilli and Michelle Maxson:** Created the figures. **David L. Moyes and Bernhard Hube:** Contributed to manuscript editing. All authors have read and approved the manuscript for submission.

DATA AVAILABILITY STATEMENT

The data that support the findings of this study are available from the corresponding author upon reasonable request.

ORCID

Mariana Blagojevic https://orcid.org/0000-0002-6085-381X
Giorgio Camilli https://orcid.org/0000-0002-6662-0072
Michelle Maxson https://orcid.org/0000-0002-1493-490X
Bernhard Hube https://orcid.org/0000-0002-6028-0425
David L. Moyes https://orcid.org/0000-0002-1657-918X
Jonathan P. Richardson https://orcid.org/0000-0001-9638-2725
Julian R. Naglik https://orcid.org/0000-0002-8072-7917

REFERENCES

Aggor, F. E. Y., Break, T. J., Trevejo-Nunez, G., Whibley, N., Coleman, B. M., Bailey, R. D., … Gaffen, S. L. (2020). Oral epithelial IL-22/STAT3 signaling licenses IL-17-mediated immunity to oral mucosal candidiasis. *Science Immunolology*, *5*(48), eaba0570. https://doi.org/10.1126/sciimmunol.aba0570

Allert, S., Forster, T. M., Svensson, C. M., Richardson, J. P., Pawlik, T., Hebecker, B., … Hube, B. (2018). *Candida albicans*-induced epithelial damage mediates translocation through intestinal barriers. *MBio*, *9*(3), e00915–18. https://doi.org/10.1128/mBio.00915-18

Baines, C. P. (2010). Role of the mitochondrion in programmed necrosis. *Frontiers in Physiology*, *1*, 156. https://doi.org/10.3389/fphys.2010.00156

Baracca, A., Sgarbi, G., Solaini, G., & Lenaz, G. (2003). Rhodamine 123 as a probe of mitochondrial membrane potential: Evaluation of proton flux through F(0) during ATP synthesis. *Biochimica et Biophysica Acta*, *1606*(1–3), 137–146. https://doi.org/10.1016/s0005-2728(03)00110-5

Bauer, T. M., & Murphy, E. (2020). Role of mitochondrial calcium and the permeability transition pore in regulating cell death. *Circulation Research*, *126*(2), 280–293. https://doi.org/10.1161/CIRCRESAHA.119.316306

Brown, G. D., Denning, D. W., Gow, N. A., Levitz, S. M., Netea, M. G., & White, T. C. (2012). Hidden killers: Human fungal infections. *Science Translational Medicine*, *4*(165), 165rv113. https://doi.org/10.1126/scitranslmed.3004404

Camilli, G., Blagojevic, M., Naglik, J. R., & Richardson, J. P. (2020). Programmed cell death: Central player in fungal infections. *Trends in Cell Biology*, *3*, 176–196. https://doi.org/10.1016/j.tcb.2020.11.005

Cao, M., Wu, Z., Lou, Q., Lu, W., Zhang, J., Li, Q., … Qian, Y. (2019). Dectin-1-induced RIPK1 and RIPK3 activation protects host against *Candida albicans* infection. *Cell Death and Differentiation*, *26*(12), 2622–2636. https://doi.org/10.1038/s41418-019-0323-8

Cerella, C., Diederich, M., & Ghibelli, L. (2010). The dual role of calcium as messenger and stressor in cell damage, death, and survival. *International Journal of Cell Biology*, *2010*, 546163. https://doi.org/10.1155/2010/546163

Dalle, F., Wachtler, B., L'Ollivier, C., Holland, G., Bannert, N., Wilson, D., … Hube, B. (2010). Cellular interactions of *Candida albicans* with human oral epithelial cells and enterocytes. *Cellular Microbiology*, *12*(2), 248–271. https://doi.org/10.1111/j.1462-5822.2009.01394.x

Drummond, R. A., Swamydas, M., Oikonomou, V., Zhai, B., Dambuza, I. M., Schaefer, B. C., … Lionakis, M. S. (2019). CARD9(+) microglia promote antifungal immunity via IL-1beta- and CXCL1-mediated neutrophil recruitment. *Nature Immunology*, *20*(5), 559–570. https://doi.org/10.1038/s41590-019-0377-2

Finkel, T., Menazza, S., Holmstrom, K. M., Parks, R. J., Liu, J., Sun, J., … Murphy, E. (2015). The ins and outs of mitochondrial calcium. *Circulation Research*, *116*(11), 1810–1819. https://doi.org/10.1161/CIRCRESAHA.116.305484

Gasparoto, T. H., Gaziri, L. C., Burger, E., de Almeida, R. S., & Felipe, I. (2004). Apoptosis of phagocytic cells induced by *Candida albicans* and production of IL-10. *FEMS Immunology and Medical Microbiology*, *42*(2), 219–224. https://doi.org/10.1016/j.femsim.2004.05.006

Goyer, M., Loiselet, A., Bon, F., L'Ollivier, C., Laue, M., Holland, G., … Dalle, F. (2016). Intestinal cell tight junctions limit invasion of *Candida albicans* through active penetration and endocytosis in the early stages of the interaction of the fungus with the intestinal barrier. *PLoS One*, *11*(3), e0149159. https://doi.org/10.1371/journal.pone.0149159

Han, B., Yao, W., Oh, Y. T., Tong, J. S., Li, S., Deng, J., … Sun, S. Y. (2015). The novel proteasome inhibitor carfilzomib activates and enhances extrinsic apoptosis involving stabilization of death receptor 5. *Oncotarget*, *6*(19), 17532–17542. https://doi.org/10.18632/oncotarget.3947

Ho, J., Wickramasinghe, D. N., Nikou, S. A., Hube, B., Richardson, J. P., & Naglik, J. R. (2020). Candidalysin is a potent trigger of alarmin and antimicrobial peptide release in epithelial cells. *Cell*, *9*(3), *699*. https://doi.org/10.3390/cells9030699

Ho, J., Yang, X., Nikou, S. A., Kichik, N., Donkin, A., Ponde, N. O., … Naglik, J. R. (2019). Candidalysin activates innate epithelial immune responses via epidermal growth factor receptor. *Nature Communications*, *10*(1), 2297. https://doi.org/10.1038/s41467-019-09915-2

Ibata-Ombetta, S., Idziorek, T., Trinel, P. A., Poulain, D., & Jouault, T. (2003). *Candida albicans* phospholipomannan promotes survival of phagocytosed yeasts through modulation of bad phosphorylation and macrophage apoptosis. *The Journal of Biological Chemistry*, *278*(15), 13086–13093. https://doi.org/10.1074/jbc.M210680200

Jemmerson, R., LaPlante, B., & Treeful, A. (2002). Release of intact, monomeric cytochrome c from apoptotic and necrotic cells. *Cell Death and Differentiation*, *9*(5), 538–548. https://doi.org/10.1038/sj.cdd.4400981

Jorgensen, I., Rayamajhi, M., & Miao, E. A. (2017). Programmed cell death as a defence against infection. *Nature Reviews. Immunology*, *17*(3), 151–164. https://doi.org/10.1038/nri.2016.147

Kabir, J., Lobo, M., & Zachary, I. (2002). Staurosporine induces endothelial cell apoptosis via focal adhesion kinase dephosphorylation and focal adhesion disassembly independent of focal adhesion kinase proteolysis. *The Biochemical Journal*, *367*(Pt 1), 145–155. https://doi.org/10.1042/BJ20020665

Kasper, L., Konig, A., Koenig, P. A., Gresnigt, M. S., Westman, J., Drummond, R. A., … Hube, B. (2018). The fungal peptide toxin candidalysin activates the NLRP3 inflammasome and causes cytolysis in mononuclear phagocytes. *Nature Communications*, *9*(1), 4260. https://doi.org/10.1038/s41467-018-06607-1

Kaufmann, W. K., & Kaufman, D. G. (1993). Cell cycle control, DNA repair and initiation of carcinogenesis. *The FASEB Journal*, *7*(12), 1188–1191. https://doi.org/10.1096/fasebj.7.12.8375618

Li, Y. Z., Li, C. J., Pinto, A. V., & Pardee, A. B. (1999). Release of mitochondrial cytochrome C in both apoptosis and necrosis induced by beta-lapachone in human carcinoma cells. *Molecular Medicine*, *5*(4), 232–239.

Moyes, D. L., Shen, C., Murciano, C., Runglall, M., Richardson, J. P., Arno, M., … Naglik, J. R. (2014). Protection against epithelial damage during *Candida albicans* infection is mediated by PI3K/Akt and mammalian target of rapamycin signaling. *The Journal of Infectious Diseases*, *209*(11), 1816–1826. https://doi.org/10.1093/infdis/jit824

Moyes, D. L., Wilson, D., Richardson, J. P., Mogavero, S., Tang, S. X., Wernecke, J., … Naglik, J. R. (2016). Candidalysin is a fungal peptide toxin critical for mucosal infection. *Nature*, *532*(7597), 64–68. https://doi.org/10.1038/nature17625

Naglik, J. R., Gaffen, S. L., & Hube, B. (2019). Candidalysin: Discovery and function in *Candida albicans* infections. *Current Opinion in Microbiology*, *52*, 100–109. https://doi.org/10.1016/j.mib.2019.06.002

O'Callaghan, K., Palagano, E., Butini, S., Campiani, G., Williams, D. C., Zisterer, D. M., & O'Sullivan, J. (2015). Induction of apoptosis in oral squamous carcinoma cells by pyrrolo-1,5-benzoxazepines. *Molecular Medicine Reports*, *12*(3), 3748–3754. https://doi.org/10.3892/mmr.2015.3832

O'Meara, T. R., Duah, K., Guo, C. X., Maxson, M. E., Gaudet, R. G., Koselny, K., … Cowen, L. E. (2018). High-throughput screening identifies genes required for *Candida albicans* induction of macrophage pyroptosis. *MBio*, *9*(4), e01581–18. https://doi.org/10.1128/mBio.01581-18

O'Meara, T. R., Veri, A. O., Ketela, T., Jiang, B., Roemer, T., & Cowen, L. E. (2015). Global analysis of fungal morphology exposes mechanisms of host cell escape. *Nature Communications*, *6*, 6741. https://doi.org/10.1038/ncomms7741

Panagio, L. A., Felipe, I., Vidotto, M. C., & Gaziri, L. C. J. (2002). Early membrane exposure of phosphatidylserine followed by late necrosis in murine macrophages induced by *Candida albicans* from an HIV-infected individual. *Journal of Medical Microbiology*, *51*(11), 929–936. https://doi.org/10.1099/0022-1317-51-11-929

Pekmezovic, M., Hovhannisyan, H., Gresnigt, M. S., Iracane, E., Oliveira-Pacheco, J., Siscar-Lewin, S., … Hube, B. (2021). *Candida* pathogens induce protective mitochondria-associated type I interferon signalling and a damage-driven response in vaginal epithelial cells. *Nature Microbiology*, *5*, 643–657. https://doi.org/10.1038/s41564-021-00875-2

Reales-Calderon, J. A., Sylvester, M., Strijbis, K., Jensen, O. N., Nombela, C., Molero, G., & Gil, C. (2013). *Candida albicans* induces pro-inflammatory and anti-apoptotic signals in macrophages as revealed by quantitative proteomics and phosphoproteomics. *Journal of Proteomics*, *91*, 106–135. https://doi.org/10.1016/j.jprot.2013.06.026

Richardson, J. P., Ho, J., & Naglik, J. R. (2018). *Candida*-epithelial interactions. *Journal of Fungi (Basel)*, *4*(1), 22. https://doi.org/10.3390/jof4010022

Richardson, J. P., Mogavero, S., Moyes, D. L., Blagojevic, M., Kruger, T., Verma, A. H., … Naglik, J. R. (2018). Processing of *Candida albicans* Ece1p is critical for candidalysin maturation and fungal virulence. *mBio*, *9*(1), e02178–17. https://doi.org/10.1128/mBio.02178-17

Richardson, J. P., Willems, H. M. E., Moyes, D. L., Shoaie, S., Barker, K. S., Tan, S. L., … Peters, B. M. (2018). Candidalysin drives epithelial signaling, neutrophil recruitment, and immunopathology at the vaginal mucosa. *Infection and Immunity*, *86*(2), e00645–17. https://doi.org/10.1128/IAI.00645-17

Rupniak, H. T., Rowlatt, C., Lane, E. B., Steele, J. G., Trejdosiewicz, L. K., Laskiewicz, B., … Hill, B. T. (1985). Characteristics of four new human cell lines derived from squamous cell carcinomas of the head and neck. *Journal of the National Cancer Institute*, *75*(4), 621–635.

Swidergall, M., Khalaji, M., Solis, N. V., Moyes, D. L., Drummond, R. A., Hube, B., … Naglik, J. R. (2019). Candidalysin is required for neutrophil recruitment and virulence during systemic *Candida albicans* infection. *The Journal of Infectious Diseases*, *220*(9), 1477–1488. https://doi.org/10.1093/infdis/jiz322

Taylor, R. C., Cullen, S. P., & Martin, S. J. (2008). Apoptosis: Controlled demolition at the cellular level. *Nature Reviews. Molecular Cell Biology*, *9*(3), 231–241. https://doi.org/10.1038/nrm2312

Tucey, T. M., Verma, J., Olivier, F. A. B., Lo, T. L., Robertson, A. A. B., Naderer, T., & Traven, A. (2020). Metabolic competition between host and pathogen dictates inflammasome responses to fungal infection. *PLoS Pathogens*, *16*(8), e1008695. https://doi.org/10.1371/journal.ppat.1008695

Uwamahoro, N., Verma-Gaur, J., Shen, H. H., Qu, Y., Lewis, R., Lu, J., … Traven, A. (2014). The pathogen *Candida albicans* hijacks pyroptosis for escape from macrophages. *mBio*, *5*(2), e00003–e00014. https://doi.org/10.1128/mBio.00003-14

Vanden Berghe, T., Linkermann, A., Jouan-Lanhouet, S., Walczak, H., & Vandenabeele, P. (2014). Regulated necrosis: The expanding network of non-apoptotic cell death pathways. *Nature Reviews. Molecular Cell Biology*, *15*(2), 135–147. https://doi.org/10.1038/nrm3737

Verma, A. H., Richardson, J. P., Zhou, C., Coleman, B. M., Moyes, D. L., Ho, J., … Gaffen, S. L. (2017). Oral epithelial cells orchestrate innate type 17 responses to *Candida albicans* through the virulence factor candidalysin. *Science Immunology*, *2*(17), eaam8834. https://doi.org/10.1126/sciimmunol.aam8834

Verma, A. H., Zafar, H., Ponde, N. O., Hepworth, O. W., Sihra, D., Aggor, F. E. Y., … Moyes, D. L. (2018). IL-36 and IL-1/IL-17 drive immunity to oral candidiasis via parallel mechanisms. *Journal of Immunology*, *201*(2), 627–634. https://doi.org/10.4049/jimmunol.1800515

Villar, C. C., Chukwuedum Aniemeke, J., Zhao, X. R., & Huynh-Ba, G. (2012). Induction of apoptosis in oral epithelial cells by *Candida albicans*. *Molecular Oral Microbiology*, *27*(6), 436–448. https://doi.org/10.1111/j.2041-1014.2012.00648.x

Villar, C. C., & Zhao, X. R. (2010). *Candida albicans* induces early apoptosis followed by secondary necrosis in oral epithelial cells. *Molecular Oral Microbiology*, *25*(3), 215–225. https://doi.org/10.1111/j.2041-1014.2010.00577.x

Vylkova, S., & Lorenz, M. C. (2017). Phagosomal neutralization by the fungal pathogen *Candida albicans* induces macrophage pyroptosis. *Infection and Immunity*, *85*(2), e00832–16. https://doi.org/10.1128/IAI.00832-16

Wagener, J., Weindl, G., de Groot, P. W., de Boer, A. D., Kaesler, S., Thavaraj, S., … Schaller, M. (2012). Glycosylation of *Candida albicans* cell wall proteins is critical for induction of innate immune responses and apoptosis of epithelial cells. *PLoS One*, *7*(11), e50518. https://doi.org/10.1371/journal.pone.0050518

Wang, X. (2001). The expanding role of mitochondria in apoptosis. *Genes & Development*, *15*(22), 2922–2933.

Wellington, M., Koselny, K., Sutterwala, F. S., & Krysan, D. J. (2014). *Candida albicans* triggers NLRP3-mediated pyroptosis in macrophages. *Eukaryotic Cell*, *13*(2), 329–340. https://doi.org/10.1128/EC.00336-13

Wu, H., Downs, D., Ghosh, K., Ghosh, A. K., Staib, P., Monod, M., & Tang, J. (2013). *Candida albicans* secreted aspartic proteases 4-6 induce apoptosis of epithelial cells by a novel Trojan horse mechanism. *The FASEB Journal*, *27*(6), 2132–2144. https://doi.org/10.1096/fj.12-214353

Ying, Y., & Padanilam, B. J. (2016). Regulation of necrotic cell death: p53, PARP1 and cyclophilin D-overlapping pathways of regulated necrosis? *Cellular and Molecular Life Sciences*, *73*(11–12), 2309–2324. https://doi.org/10.1007/s00018-016-2202-5

Zakikhany, K., Naglik, J. R., Schmidt-Westhausen, A., Holland, G., Schaller, M., & Hube, B. (2007). In vivo transcript profiling of *Candida albicans* identifies a gene essential for interepithelial dissemination. *Cellular Microbiology*, *9*(12), 2938–2954. https://doi.org/10.1111/j.1462-5822.2007.01009.x

Zong, W. X., & Thompson, C. B. (2006). Necrotic death as a cell fate. *Genes & Development*, *20*(1), 1–15. https://doi.org/10.1101/gad.1376506

SUPPORTING INFORMATION

Additional supporting information may be found online in the Supporting Information section at the end of this article.

How to cite this article: Blagojevic, M., Camilli, G., Maxson, M., Hube, B., Moyes, D. L., Richardson, J. P., & Naglik, J. R. (2021). Candidalysin triggers epithelial cellular stresses that induce necrotic death. *Cellular Microbiology*, e13371. https://doi.org/10.1111/cmi.13371